

ChemSusChem

Supporting Information

Cytochrome c* Reductase is a Key Enzyme Involved in the Extracellular Electron Transfer Pathway towards Transition Metal Complexes in *Pseudomonas Putida

Bin Lai,* Paul V. Bernhardt, and Jens O. Krömer*© 2020 The Authors. Published by Wiley-VCH GmbH. This is an open access article under the terms of the Creative Commons Attribution Non-Commercial License, which permits use, distribution and reproduction in any medium, provided the original work is properly cited and is not used for commercial purposes.

List of supplementary figures for main text

Figures	Descriptions
Figure S1	The schematic of protein synthesis machinery (A) and their abundance changes during the BES batch (B).
Figure S2	The BES fermentation of <i>P. putida</i> F1 with sodium azide and ferricyanide. A) the current, biomass and pH profile; B) the metabolic product spectrum.
Figure S3	The growth properties of <i>P. putida</i> F1 in DM9 medium with different rotenone concentrations.
Figure S4	The abiotic interaction of rotenone with ferri-/ferrocyanide tested in BES.
Figure S5	The growth properties of <i>P. putida</i> F1 in DM9 medium with different antimycin A concentrations.
Figure S6	The abiotic interaction between antimycin A and ferricyanide (A) and the UV-vis spectrum of ferricyanide, rotenone and antimycin A (B).
Figure S7	Cyclic voltammetry tests of BES reactor with and without ferricyanide, <i>P. putida</i> F1 cells, antimycin A and magnetic stirring.
Figure S8	Pictures of BES reactors with the cobalt mediator at different redox status.
Figure S9	The UV-vis spectrum of different redox status of the cobalt mediator and the free pyridine (<i>bpy</i>) legend.

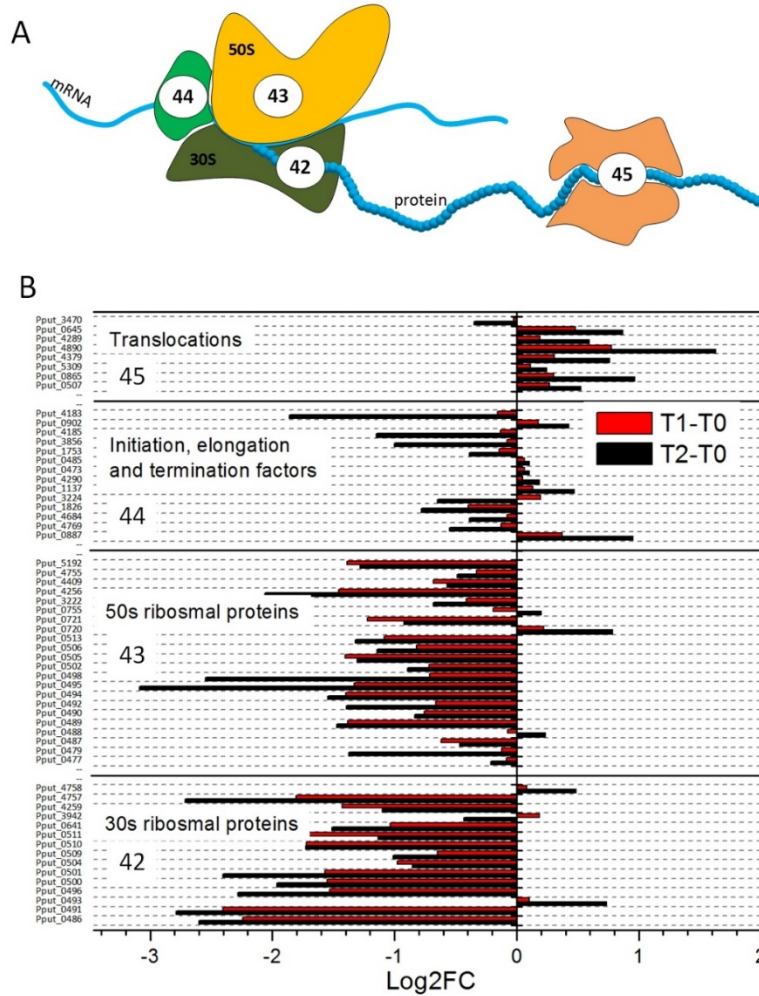


Figure S1. **The schematic of protein synthesis machinery (A) and their abundance changes during the BES batch (B).** T0: the time of reactor inoculation; T1: mid-phase of the batch; T2: end of the batch. Log2FC: the log2 transformation of fold changes (FC) of protein abundance calculated using MSstat in RStudio.

Majority of the proteins involved in the protein synthesis were down-regulated during the BES batch, indicating the protein synthesis activity was largely restricted. The upregulation of translocations units may suggest the active synthesis of some essential proteins required for cell maintenance.

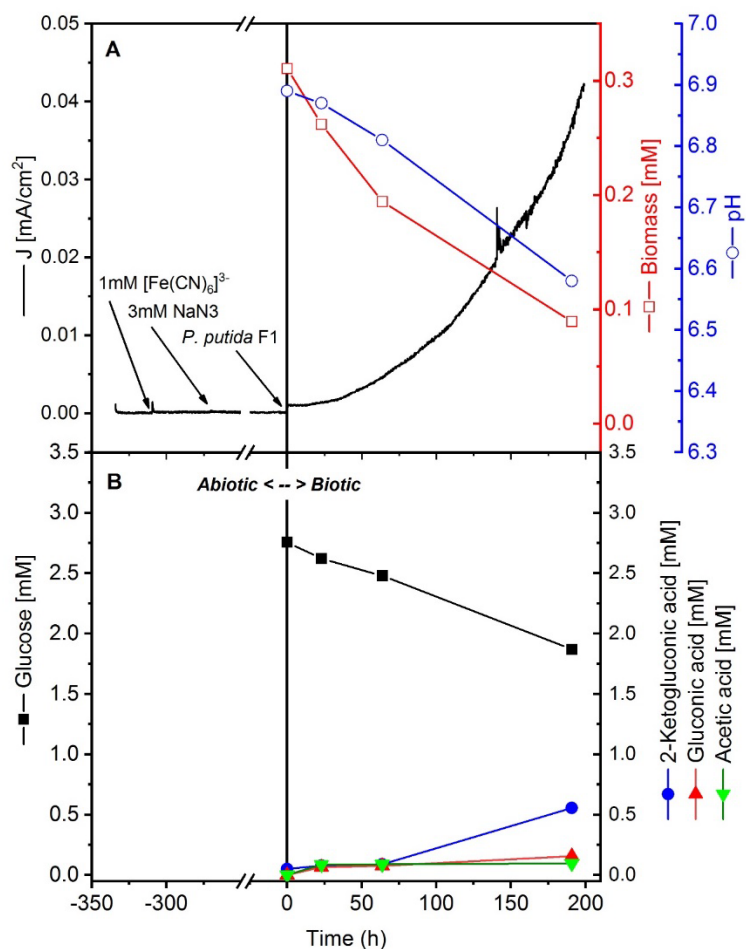


Figure S2. The BES fermentation of *P. putida* F1 with sodium azide and ferricyanide. A) the current, biomass and pH profile; B) the metabolic product spectrum.

This batch is to check if there is any chemical reaction between sodium azide and ferricyanide. Therefore, the NaN₃ was added after the ferricyanide but before inoculation. A abiotic phase of nearly 350h was kept in this case for long-term capability test. As seen in the figure, there is no visible change in the current profile upon adding NaN₃ and also after inoculation, the *P. putida* F1 can export electron to the mediator/electrode as in normal cases without NaN₃. The metabolites spectrum also had no detectable changes in this batch. All these demonstrated that NaN₃ has no chemical interaction with ferricyanide.

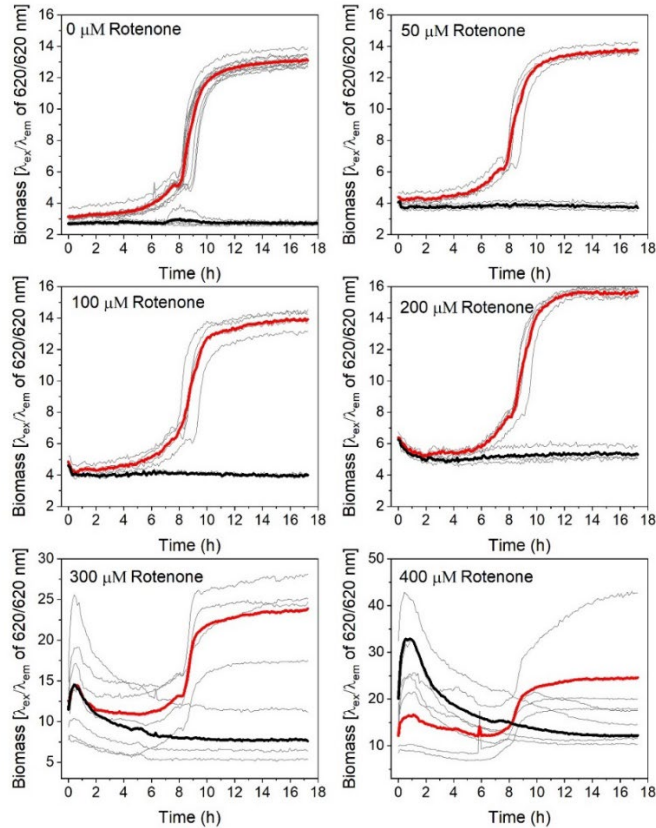


Figure S3. The growth properties of *P. putida* F1 in DM9 medium with different rotenone concentrations. The tests were conducted with Biolector Pro cultivation system. The grey lines refer to the raw data, while the red for averaged data of bio-group and the black for abiotic controls.

Rotenone stock solutions of 120mM were made in DMSO, and 0.5, 1, 2, 3 and 4 μ l stock solutions were added into each well (1200 μ l final volume) on the microplate to achieve the respective desired concentrations from 50 to 400 μ M. For the controls of 0 μ M, different amount pure DMSO (from 0.5-4 μ l) DMSO were added, corresponding to the volumes of different rotenone concentrations. The concentration of DMSO in the medium ranged from 0.04% to 0.33% v/v, which are much lower compared to the known concentrations that would induce quorum sensing effects for *P. putida* (10% DMSO¹) and even *P. aeruginosa* (\geq 1% DMSO^{2,3}). No concentration-dependent effects of DMSO on cell growth were observed. All these suggested no quorum sensing effects induced by DMSO under the tested conditions in this paper.

As seen in the figure, strong abiotic background could be detected for the rotenone concentrations of 300 μ M and 400 μ M, which was due to the fact that the solutions were too cloudy.

¹ Bodini, S. F., et al. (2009). Letters in Applied Microbiology 49(5): 551-555.

² Guo, Q., et al. (2016). Antimicrobial Agents and Chemotherapy 60(12): 7159-7169.

³ Malešević, M., et al. (2019). Scientific Reports 9(1): 16465.

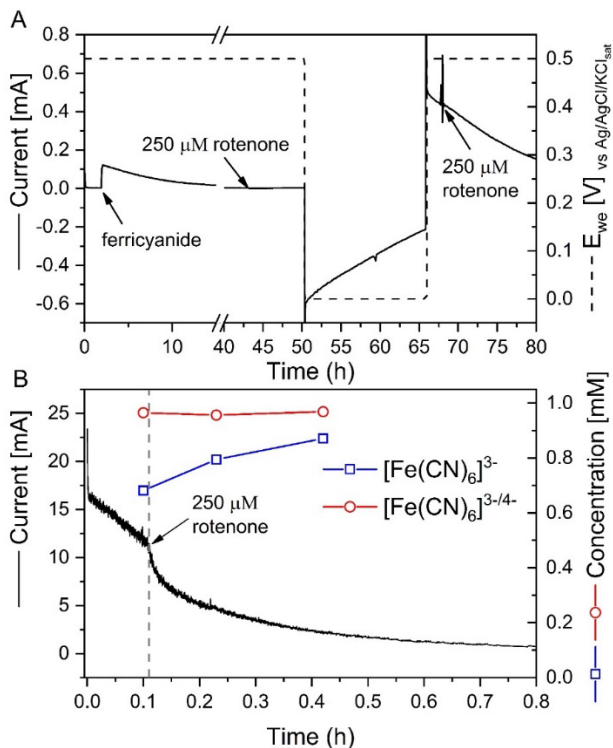


Figure S4. The abiotic interaction of rotenone with ferri-/ferrocyanide tested in BES. A) rotenone was injected twice while only ferricyanide was presented or a mixture of ferricyanide and ferrocyanide was existed in the medium. B) a new batch where rotenone was added to a mixture of ferricyanide and ferrocyanide.

Under atmosphere conditions, the stock solution of ferricyanide is in fact a mixture of ferricyanide and ferrocyanide. Therefore, the first rotenone injection in batch A was performed about 40h after adding ferricyanide while no significant oxidation current could be detected. As presented in Figure S4A, there was no change in the current output after adding rotenone, confirming there was chemical interaction between rotenone and ferricyanide. Afterwards, ferricyanide was reduced to ferrocyanide by changing the redox potential and then the working electrode potential was changed back to 0.697V vs SHE to oxidize the ferrocyanide in the mixture. A second injection of rotenone was performed to check if rotenone could affect the oxidation of ferrocyanide. There were no visible changes in the current output as well, suggesting rotenone did not react with ferrocyanide as well. The new batch in the Figure S4B was conducted concerning the electrode surface was coated by rotenone already before the second injection of rotenone. Therefore, same approach as batch A was applied to get a mixture of ferricyanide and ferrocyanide in the medium first and subsequently the rotenone was injected. The current output was lowered down upon the injection, but this effect was quite likely due to the absorption of excessive rotenone on the electrode surface since the overall concentration of ferricyanide and ferrocyanide was stable in the medium, validating that rotenone has no chemical reaction with both ferricyanide and ferrocyanide.

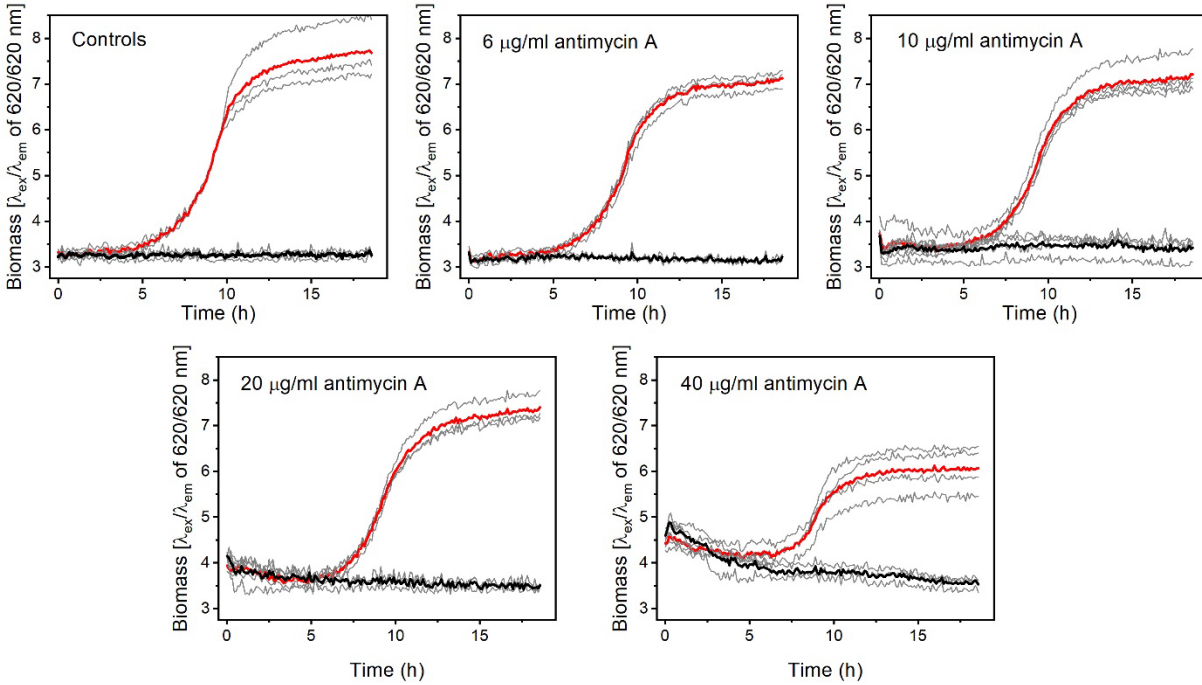


Figure S5. The growth properties of *P. putida* F1 in DM9 medium with different antimycin A concentrations. The light grey lines were raw data of three or four replicates. The red lines were the averaged data for biologic group and the black lines referred to the averaged data of abiotic controls for each condition.

The stock solution of antimycin A was made in pure ethanol. Preliminary experiments showed ethanol could also be used as carbon source for cell growth. Therefore, the concentration of antimycin A in the stock solution was adjusted to respective value to ensure same amount of ethanol was added under each condition. In details, the stock solutions of antimycin A were adjusted to 1.5, 3, 5, 10 and 20 $\mu\text{g}/\mu\text{l}$, and thus 2.4 μl stock solution was added into each well on the microplate. In the controls, 2.4 μl pure ethanol was used.

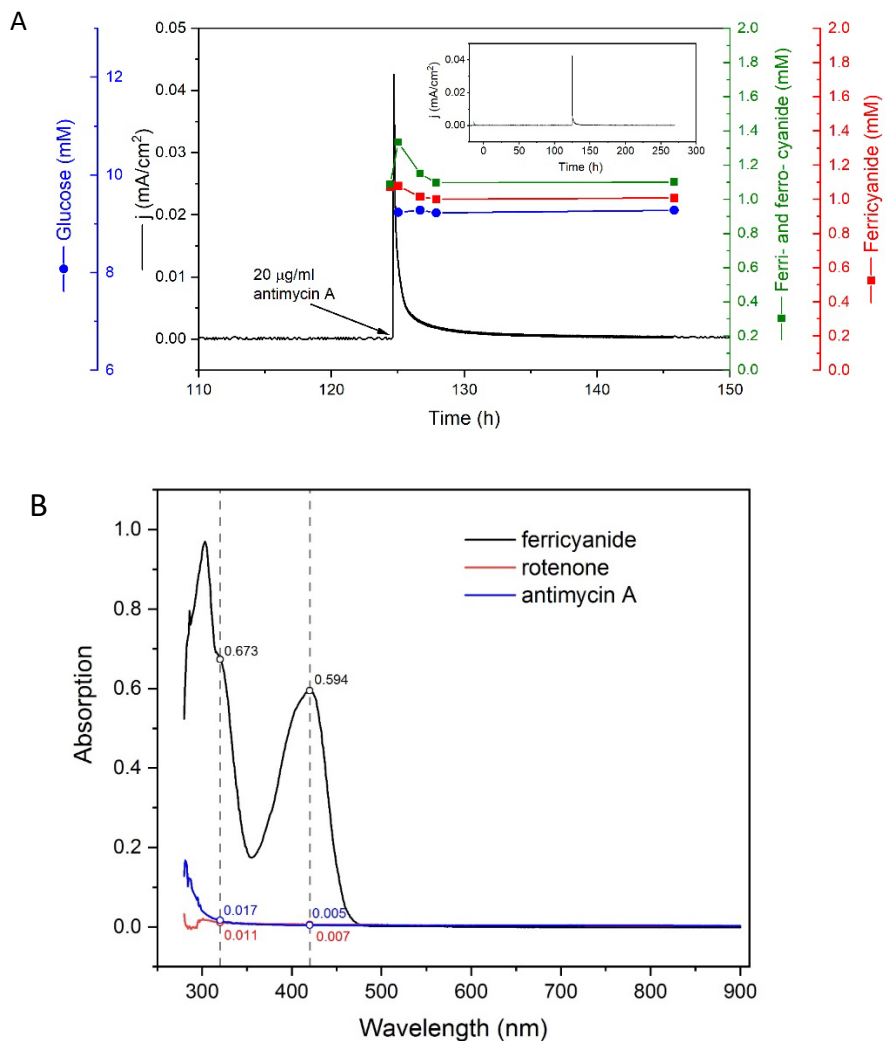


Figure S6. The abiotic interaction between antimycin A and ferricyanide (A) and the UV-vis spectrum of ferricyanide, rotenone and antimycin A (B).

As seen in Figure S6A, an anodic current was detected after injecting antimycin A into M9 medium containing ferricyanide. The concentration of ferricyanide was also decreased and could not be recovered afterwards. These results indicated a chemical reaction between antimycin A and ferricyanide.

The Figure S6B showed the rotenone and antimycin A should not affect the quantification of ferricyanide under 420nm, which excluded the possibility that the decrease of ferricyanide in S6A was due to measurement error.

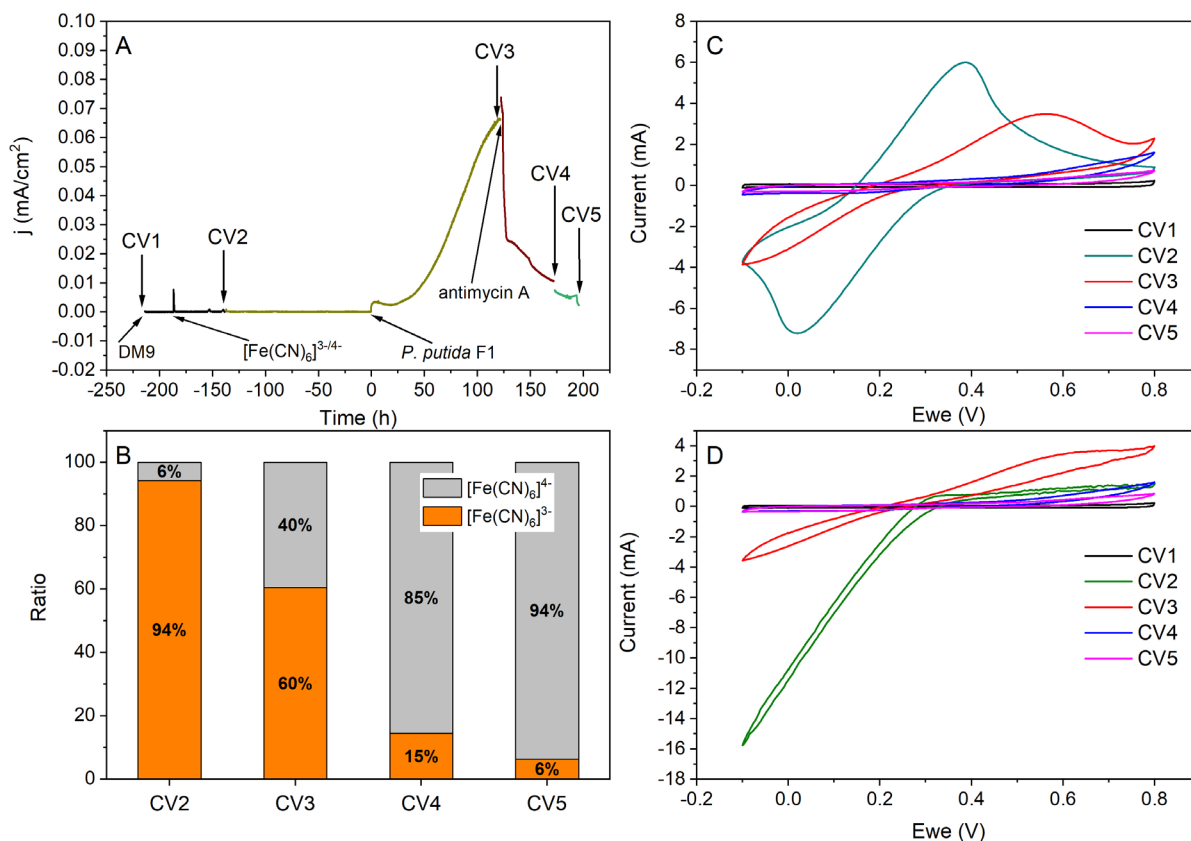


Figure S7. Cyclic voltammetry tests of BES reactor with and without ferricyanide, *P. putida* F1 cells, antimycin A and magnetic stirring. A) The 5 time points along the BES batch where the cyclic voltammetry tests were conducted. CV1, DM9 blank medium; CV2, DM9 + mediator; CV3, DM9 + mediator + *P. putida* F1; CV4: DM9 + mediator + *P. putida* F1 + antimycin A; CV5: DM9 + mediator + *P. putida* F1 + antimycin A. B) The measurements of ferricyanide and ferrocyanide at the respective time points for cyclic voltammetry tests. Data was normalized to the measured total concentrations, which did not show significant changes along the batch. Grey color is for the reduced ferrocyanide, and orange for the oxidised ferricyanide. C) Cyclic voltammograms for CV1-CV5 without magnetic stirring. D) Cyclic voltammograms for CV1-CV5 with magnetic stirring (400rpm). Scanning rates were 10mV/s for all measurements.

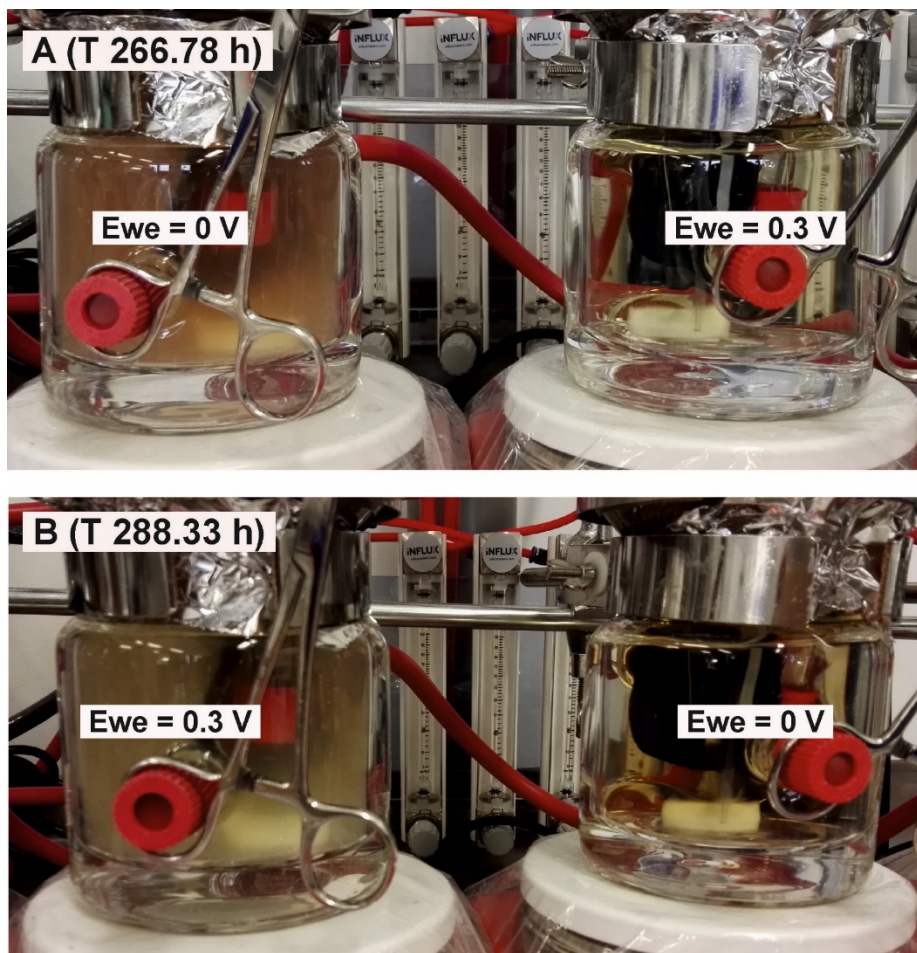


Figure S8. Pictures of BES reactors with the cobalt mediator at different redox status. The left was a reactor with *P. putida* F1 cells, and the right reactor was the abiotic control.

Some colour changes could be seen while the cobalt mediator was at different redox status. The solution became yellowish while the mediator was in the fully oxidized form, and the colour would change to brown-red for the reduced form. This could be used to qualitatively address the redox form for this chemical in the medium, but not quantitatively. The potential listed in the picture were against silver electrode ($\text{Ag}/\text{AgCl}/\text{KCl}_{\text{sat}}$)

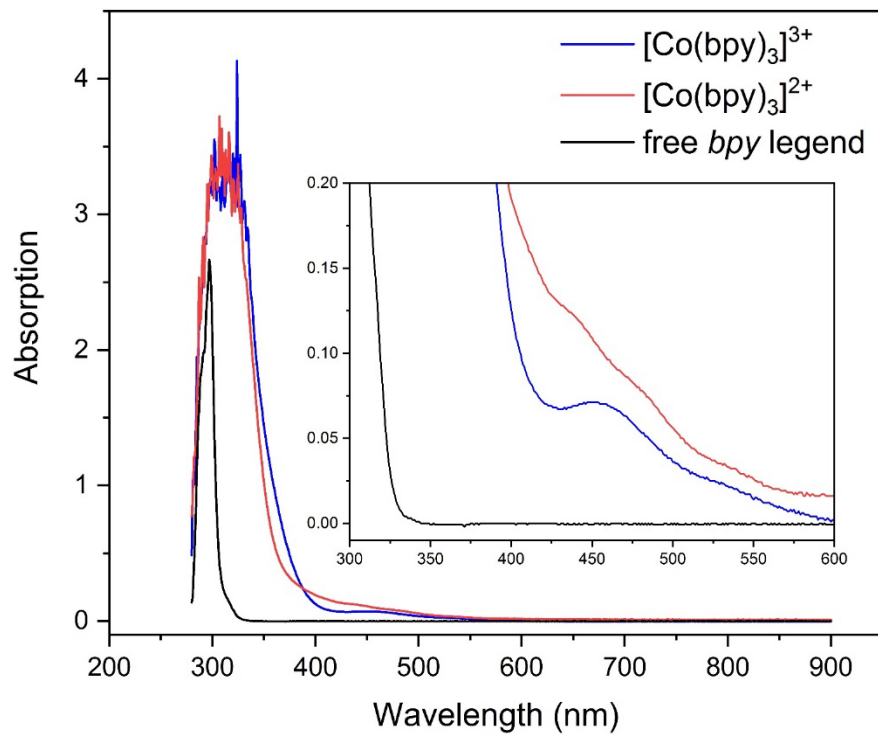


Figure S9. The UV-vis spectrum of different redox status of the cobalt mediator and the free pyridine (*bpy*) ligand.

The different redox status of this compound was achieved by oxidizing or reducing the compound in an electrochemical cell until no oxidizing or reducing current could be detected. The samples were taken for UV-vis spectrum scanning. The spectra of $[\text{Co}(\text{bpy})_3]^{3+}$ and $[\text{Co}(\text{bpy})_3]^{2+}$ showed no significant difference and thus it would not be feasible to develop any colorimetric assay to distinguish and quantify the different redox status of this compound.